NASA TECHNICAL NOTE

NASA TN D-5404

C.1

NASA TN D-5404

EXPERIMENTAL MEASUREMENTS OF EXPANDING STORABLE-PROPELLANT PRODUCTS SIMULATED BY COMBUSTION OF GASEOUS REACTANTS

by Robert Friedman, Raymond E. Gaugler, and Erwin A. Lezberg

Lewis Research Center
Cleveland, Ohio

NATIONAL AERONAUTICS AND SPACE ADMINISTRATION • WASHINGTON, D. C. • SEPTEMBER 1969

EXPERIMENTAL MEASUREMENTS OF EXPANDING STORABLE-PROPELLANT PRODUCTS SIMULATED BY COMBUSTION OF GASEOUS REACTANTS

By Robert Friedman, Raymond E. Gaugler, and Erwin A. Lezberg

Lewis Research Center
Cleveland, Ohio

NATIONAL AERONAUTICS AND SPACE ADMINISTRATION

For sale by the Clearinghouse for Federal Scientific and Technical Information
Springfield, Virginia 22151 – CFSTI price $3.00

ABSTRACT

The storable system, 50-weight-percent unsymmetrical dimethylhydrazine and 50-percent hydrazine fuel with nitrogen tetroxide oxidizer, was simulated by combustion of hydrogen and methane with oxygen-enriched air in order to focus attention on the non-equilibrium expansion process. Static temperatures and pressures for the expanding combustion products, simulating a storable-propellant equivalence ratio range of 0.9 to 1.4, were measured in a 5.6-area-ratio conical nozzle. Temperatures were nearly independent of oxidant-fuel ratio and were close to those calculated for frozen-expansion and kinetic analyses.

EXPERIMENTAL MEASUREMENTS OF EXPANDING STORABLE-PROPELLANT PRODUCTS SIMULATED BY COMBUSTION OF GASEOUS REACTANTS

by Robert Friedman, Raymond E. Gaugler, and Erwin A. Lezberg

Lewis Research Center

SUMMARY

The nonequilibrium expansion of the combustion products of the storable-propellant system, 50-weight-percent unsymmetrical dimethylhydrazine and 50-percent hydrazine fuel with nitrogen tetroxide oxidizer, was experimentally investigated. The investigation was conducted at 3.8×10^5 and 4.8×10^5 newtons per square meter (3.7 and 4.7 atm) in a 5.6-area-ratio, nominal Mach 3, axisymmetric, conical nozzle. A relatively new technique was used in which the storable-propellant combustion products were simulated by using the reactants methane, hydrogen, oxygen, and air. The relative flow rates of the simulating propellants and the oxidant preheat necessary for duplication of storable-propellant product composition and enthalpy were readily computed. In practice the simulation technique proved feasible, and calculations showed that the effect on the experimental results of small deviations from accurate simulation could be neglected. The experimental measurements of static temperature and static pressure were made at conditions simulating oxidant-fuel mass ratios (O/F) of 1.6 to 2.5 (equivalence ratios of 1.4 to 0.9). Temperatures were nearly independent of O/F over this range and were close to those calculated by frozen-expansion and kinetic analyses.

INTRODUCTION

Chemical nonequilibrium flow in nozzles arises from the atoms and free radicals that are produced in high-temperature combustion. These species can recombine, but the recombination reaction rates are often slow with respect to the residence time in the nozzle, and shifting equilibrium cannot be maintained during the nozzle flow. Energy release in such cases is less than predicted for equilibrium expansions, and this nonequilibrium flow can cause appreciable thrust losses in ramjet and rocket engines.

Experimental measurements of nozzle recombination processes have been made at Lewis for hydrogen and air (refs. 1 and 2) to supplement and confirm analyses based on laboratory reaction rates. Reaction rates reported in the literature for hydrogen-oxygen systems vary by an order of magnitude or more, but the experiments showed satisfactory agreement of experimental and analytical nozzle temperatures and engine performance.

In this investigation, nozzle recombination studies were extended to more complicated propellant systems containing carbon, hydrogen, oxygen, and nitrogen. The liquid storable propellants, 50-weight-percent unsymmetrical dimethylhydrazine (UDMH) and 50-percent hydrazine fuel with nitrogen tetroxide oxidizer, are of particular interest because of their application to modern space engines. Theoretical analyses of nonequilibrium expansion of this propellant system have previously been reported by several investigators (refs. 3 to 5). In addition, laboratory measurements of the performance of these propellants in engines were conducted by Aukerman and Trout (ref. 6), but the separation of total losses into kinetic, combustion, and aerodynamic inefficiencies could only be assumed from the prior analyses. In the present study, a relatively new technique was used that isolated the expansion from the combustion process. Exhaust products identical to those produced by the complete combustion of the storable-propellant system were generated by combustion of gaseous methane, hydrogen, oxygen, and air. These gaseous reactants burned at nearly 100-percent efficiency, and the problems of combustor injection, vaporization, instability, and the like were eliminated. This simulation depended on a prior calculation of the combustion products and enthalpy for given operating conditions. This method had also been proposed by Sheeran (ref. 7) and used experimentally in at least one instance for simulation of kerosene by acetylene and hydrogen (ref. 8). The simulation technique was thoroughly analyzed in this investigation to determine the sensitivity of the expansion-temperature results to errors in the simulating-reactant composition and properties. Experimental results obtained by using the simulating reactants were compared to theoretical analyses based on the storable propellants.

This report presents results of analysis and experiments on the expansion of the combustion products of simulated storable propellants at combustion-chamber pressures of 3.8×10^5 and 4.8×10^5 newtons per square meter (3.7 and 4.7 atm) and a range of oxidant-fuel mass ratios (O/F) of 1.6 to 2.5 (equivalence ratios of 1.4 to 0.9). Measurements were made of static temperature and pressure in a 5.6-area-ratio, nominal Mach 3, axisymmetric nozzle placed in a connected-pipe facility.

APPARATUS

Air from the laboratory system and oxygen from a cylinder trailer were metered through standard orifices, heated in an aluminum-oxide pebble-bed storage heat exchanger, and then passed into a water-cooled combustion chamber where the fuel was

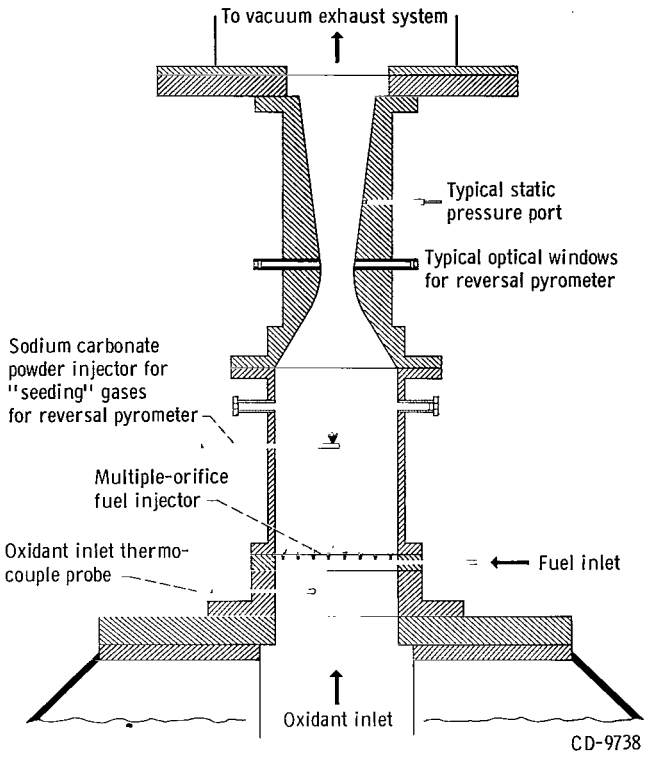

Figure 1. - Sketch of combustion chamber and test nozzle.

introduced and ignited spontaneously. The combustion products expanded through a supersonic nozzle and were finally cooled and ducted to the laboratory exhaust system. The combustion chamber and test nozzle are illustrated in figure 1. More details on the pebble-bed heater can be found in previous reports by Lezberg and Lancashire (refs. 9 and 10).

The combustion chamber was a cylinder, 30.7 centimeters in diameter and 46.5 centimeters long. Fuel was injected into the combustion chamber through water-cooled fuel-injection tubes arranged to distribute the fuel uniformly. The fuel was a mixture of natural gas (93.6-wt. % methane) and hydrogen; a typical analysis is shown in table I. The fuel blend was stored at high pressure in a cylinder trailer with enough capacity for two to four test runs.

The test nozzle was a conical, axisymmetric nozzle with a 30° half-angle converging section and a 7° half-angle diverging section and a 17.7-centimeter radius-of-curvature throat. The throat inside diameter was 7.94 centimeters, and the diverging section was 46.7 centimeters long. The inside walls were water-cooled and were constructed of copper; except for material and minor changes, the nozzle was built to specifications similar to those described in reference 1. The equivalent one-dimensional exit area ratio of the nozzle, corrected for boundary-layer growth as determined by heated-air nonburning calibrations, was 5.6. The nozzle had five pairs of nitrogen-purged, 1.3-

TABLE I. - TYPICAL ANALYSIS OF HYDROGEN

AND NATURAL GAS FUEL MIXTURE

Constituent	Volume percent
Hydrogen	66.80
Methane	30.75
Ethane	1.13
Carbon dioxide	.49
Helium	.35
Nitrogen	.25
Propane	.19
Butanes and higher hydrocarbons	.04
Total	100.00

centimeter-diameter optical ports located at diverging area ratios of 1.30, 1.65, 2.05, 2.50, and 3.60. Static-pressure taps were drilled normal to the nozzle wall.

Combustion products were seeded with sodium carbonate powder introduced by a water-cooled injector located in the combustion chamber, 27.4 centimeters downstream of the fuel-injector plane. This produced a beam of seeded gases flowing downstream and spreading slowly radially from the nozzle centerline. Static temperatures of the expanding exhaust products were measured by a spectral-line reversal pyrometer (described by Buchele in ref. 11), which automatically balanced the seeded-gas radiation against that of a current-controlled tungsten ribbon lamp. Temperatures were computed from an initial calibration of the lamp brightness temperature as a function of lamp current, using an optical pyrometer. The detector, lamp, and optics were mounted on an external U-shaped platform that straddled the nozzle and was moved successively to each of the optical port locations during a test run.

Optical ports were also located in the combustion chamber, 10 centimeters downstream of the sodium carbonate seeding injector. In this distance the beam of seeded gases spread very little, and temperature profiles across the combustion chamber were measured by traversing the sodium carbonate injector parallel to the pyrometer light axis (ref. 12). For this measurement, it was necessary to replace the tungsten ribbon lamp by a carbon arc source for higher reference temperatures (ref. 11).

PROCEDURE

The simulation of the storable propellants at desired oxidant-fuel mass ratios (O/F) required three controls: (1) the composition of the fuel mixture, (2) the relative rates of fuel and oxygen flows to airflow, and (3) the preheat of the oxidants. Tests were con-

ducted principally at a combustion-chamber pressure of 3.8×10^5 newtons per square meter (3.7 atm), but some runs were taken at 4.8×10^5 newtons per square meter (4.7 atm). After airflow was established, the ratios of fuel and oxygen flows to airflow were regulated by hydraulically operated flow valves to simulate O/F values ranging from 1.6 to 2.5. The flow rates were computed by a digital computer program using inputs from transducer signals. The fuel trailer was refilled several times in the course of the investigation, and the composition of the fuel blend varied slightly each time from the nominal composition specified in table I. Each fuel blend was analyzed by a mass spectrometer, and the actual analysis was used for calculation of the flow rates required for simulation of desired O/F values. The oxidants were preheated by the pebble-bed heater, which was operated at about half its maximum temperature capability. A tolerance of about 100 K was accepted in establishing oxidant-inlet temperatures with respect to prescribed values for the simulation, because it was difficult to adjust the storage heater output more precisely. During the time required for a run, only a slight drop in oxidant-inlet temperature occurred, no more than 20 K. The oxidant-inlet temperature was measured by a single shielded, thermocouple made of platinum - 13-percent rhodium and platinum.

SIMULATION

Calculations

The equilibrium combustion of 50-weight-percent hydrazine (N_2H_4) and UDMH ($C_2H_8N_2$) fuel with nitrogen tetroxide (N_2O_4) oxidizer is written on the basis of 1 mole of fuel:

$$0.6522\ N_2H_4 + 0.3478\ C_2H_8N_2 + \frac{O/F}{2.245}(1.0217\ N_2O_4) \rightarrow \text{Products}$$

where O/F is the oxidant-fuel mass ratio (2.245 for stoichiometric combustion). The products of combustion consist of H_2O, N_2, CO, CO_2, OH, O_2, H_2, H, NO, and O, the proportions being a function of the O/F and the initial properties of the reactants. There are no compounds among these products with N-H or C-H bonds since the hydrazine and UDMH molecules are dissociated in the initial phases of combustion. Calculations show that the same products would then be produced by a mixture of methane, hydrogen, oxygen, and air, which would supply the necessary C, H, O, and N atoms.

Thus, the simulation of the storable-propellant products would proceed:

$$0.6956\ CH_4 + 1.3044\ H_2 + 1.000\ N_2 + \frac{O/F}{2.245}(1.0217\ N_2 + 2.0434\ O_2) \rightarrow \text{Products}$$

Note that nitrogen appears in both the fuel and oxidant, in accordance with the composition of the storable propellants.

The simulation of combustion products also requires control of the properties of the reactants as well as matching the atomic constituents. The storable propellants, which are usually room-temperature liquids, have higher enthalpies than the less complex gaseous propellants simulating them. Matching the combustion products for the two sets of reactants required supplying additional energy to the gaseous propellants, which was conveniently performed by preheating the oxidant (oxygen and air). Standard equilibrium combustion programs (ref. 13) were used for calculating the required oxidant-inlet temperatures, and results are shown in figure 2. The oxidant-inlet temperature is a function of the simulated O/F, decreasing as the O/F increases, that is, as the proportion of oxidant increases.

Tables of oxidant preheat and fuel-oxidant proportions were prepared by stoichiometric calculations and the equilibrium-combustion program, for simulation of storable-propellant operation over a range of O/F from 1.6 to 2.5 (equivalence ratios of 1.4 to 0.9) at two combustion-chamber pressures. An example of the close match of properties and composition of the products of storable and simulating propellants is shown in

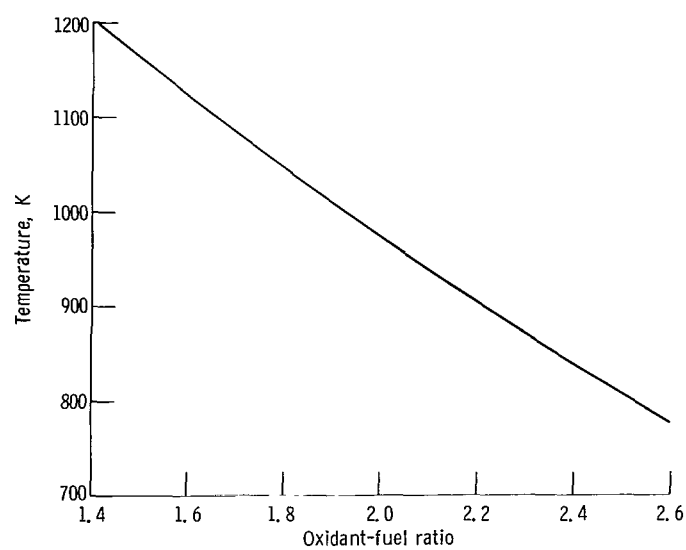

Figure 2. - Calculated oxidant preheat temperatures necessary to simulate storable-propellant combustion at combustion-chamber pressure of 3.8×10^5 newtons per square meter (3.7 atm).

TABLE II. - COMPARISON OF CALCULATED EQUILIBRIUM PROPERTIES AND COMPOSITION OF COMBUSTION PRODUCTS

[Chamber pressure, 3.8×10^5 N/sq m (3.7 atm); oxidant-fuel ratio, 1.6.]

Property	Storable propellants	Simulating propellants[a]
Temperature, K	2992	2991
Enthalpy,[b] J/kg	2.807×10^5	2.561×10^5
Enthalpy,[b] cal/g	67.1	61.2
Gamma (isentropic exponent for reacting mixture)	1.140	1.139
Molecular weight	20.48	20.54
Composition, mole fraction:		
He	0	0.0013
CO	0.0973	0.0961
CO_2	0.0337	0.0343
H	0.0294	0.0290
H_2	0.1364	0.1330
H_2O	0.3441	0.3456
N_2	0.3234	0.3243
NO	0.0039	0.0040
O	0.0033	0.0034
O_2	0.0033	0.0035
OH	0.0251	0.0255

[a]Oxidant-inlet temperature, 1100 K.

[b]Enthalpy based on zero value for reference elements at 298.15 K.

table II. For this comparison, the simulating oxidant-inlet temperature was rounded to 1100 K rather than the correct 1120 K, and natural gas composition was used instead of pure methane for the fuel. These adjustments represent a practical example; but, nevertheless, it is seen that storable and simulating combustion-product properties and compositions agree very closely. Enthalpy is based on zero enthalpy at 298.15 K for reference elements. The difference of 5.9 calories per gram in enthalpy appears to be an appreciable fraction of the enthalpy because of this reference base, but this difference is very minor, being equivalent to 1 K.

Combustion-Chamber Profiles

It was assumed in the calculation of simulation of combustion-chamber products that the combustion process was in chemical equilibrium. Experimental evidence of combustion-chamber equilibrium was obtained in this study by measurement of the

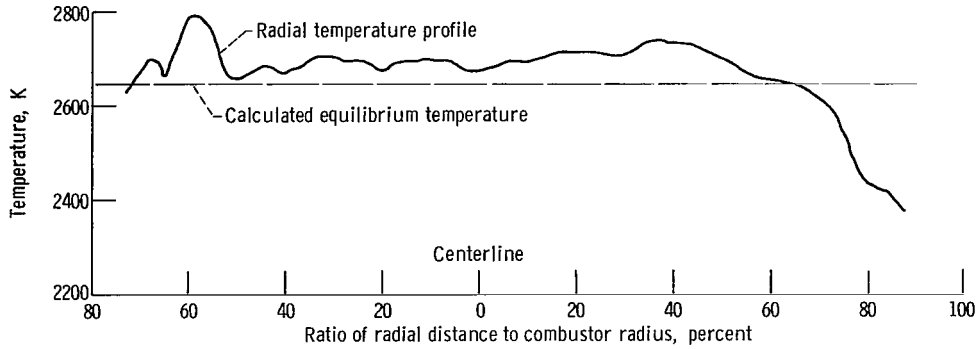

Figure 3. - Combustor-exit temperature profile for combustion of methane-hydrogen mixture and air. Air-inlet temperature, 1180 K; combustion-chamber pressure, 3.8×10^5 newtons per square meter; equivalence ratio, 0.98.

combustion-chamber outlet temperature profiles. An example of a radial combustion-chamber profile is shown in figure 3, for combustion at 3.8×10^5 newtons per square meter (3.7 atm), 1180 K air-inlet temperature, and an equivalence ratio of 0.98. These measurements were made for combustion of the hydrogen-methane fuel blend with air only, to keep combustion temperatures in the range of the carbon-arc reference light source. The radial temperature profile shown in figure 3 is flat and agrees well with the calculated equilibrium combustion temperature, indicated by the broken line. Although these results were obtained for runs without oxygen addition, the equilibrium combustion shown by these tests was regarded as typical of all the simulating-propellant operating conditions.

In storable-propellant systems, as pointed out by Sawyer (ref. 14), there may be conditions where combustion is nonequilibrium. In such cases, excess hydrazine decomposes to form ammonia, and the simulation procedure of this study, which does not supply reactants with N-H bonds, would fail to reproduce the combustion products. Nonequilibrium combustion for the storable-propellant system is likely, however, only where considerable proportions of excess reactants exist, and the studies herein were confined to O/F values near stoichiometric, in the equivalence ratio range of 0.9 to 1.4.

Feasibility of Simulation

While the theoretical calculation of the simulation technique was one of the goals of this investigation, the application of this method to experimental measurements of the expansion process was equally important. Small compromises in choosing the reactant composition and properties were unavoidable in the experiments. The possible influence of these effects on the experimental data is discussed in connection with the experimental results.

In general, it appeared that simulation of combustion-chamber products by combustion of simple reactants might also hold promise in expansion studies of other propellant combinations.

ANALYSIS

Static temperatures of the expanding combustion products were predicted by the use of a standard thermochemical program (ref. 13) for two limiting expansion modes that require no chemical reaction-rate information: (1) equilibrium expansion, in which the chemical reaction rates are infinitely fast and the species are always in chemical equilibrium; and (2) frozen expansion, in which chemical reaction rates are zero, and the composition of the exhaust products is fixed at the equilibrium combustion-chamber product composition. Comparisons with the data were also made using kinetic, or finite chemical reaction-rate calculations. The solution of the simultaneous differential equations of fluid dynamics and chemical reaction is extremely complicated, although efficient numerical techniques are available. Simplified approximate methods are frequently accurate enough for the kinetic expansion calculation; and, in this investigation, theoretical kinetic comparisons were made using the approximate analysis of Franciscus and Healy (ref. 15). This simplified method uses a modification of the Bray criterion (ref. 16), wherein the expansion is considered to be in equilibrium up to a certain nozzle station (the "sudden-freezing" point) and frozen thereafter. Chemical reaction-rate information is needed only to establish the sudden-freezing-point location, which was defined as the area ratio where the rate of decrease in number of moles of radicals or atoms is equal to the rate of recombination. For the storable-propellant system, only the three-body recombination reactions contribute to the change in number of moles. The important three-body reactions are

$$H + OH + M \rightarrow H_2O + M \qquad k_f = 7.50\times10^{19} \times T^{-1} \qquad \text{(I)}$$

$$H + H + M \rightarrow H_2 + M \qquad k_f = .30\times10^{19} \times T^{-1} \qquad \text{(II)}$$

$$O + O + M \rightarrow O_2 + M \qquad k_f = .99\times10^{19} \times T^{-1} \qquad \text{(III)}$$

$$O + H + M \rightarrow OH + M \qquad k_f = .40\times10^{19} \times T^{-1} \qquad \text{(IV)}$$

$$H + O_2 + M \rightarrow HO_2 + M \qquad k_f = 2.7\times10^{19} \times T^{-1} \qquad \text{(V)}$$

where M is any third body, T is temperature in K, and k_f is the forward reaction

rate in the units commonly used ($K\text{-}cm^6/mole^2/sec$). These rates are essentially those used in a previous nozzle expansion study (ref. 2) with a few revisions based on reference 17 and other later sources. At most conditions, the overall reaction rate and heat release are controlled by only reactions I and V (refs. 2 and 17). The principal carbon reaction

$$CO + OH \rightarrow CO_2 + H \qquad \text{(VI)}$$

may be neglected because it has negligible influence on nozzle temperatures due to its small energy release with respect to the H and O recombinations of reactions I to V.

EXPERIMENTAL RESULTS

Nozzle Measurements

Some of the experimental static temperatures measured in the test nozzle at a combustion-chamber inlet pressure of 3.8×10^5 newtons per square meter are plotted in figures 4(a) to (d) for simulated oxidant-fuel ratios of 1.6, 2.0, 2.25, and 2.4. For comparison with the experimental data, the plots show the theoretical equilibrium, frozen, and kinetic expansion temperatures. For the kinetic analysis, the results of an approximate analysis (ref. 15) are shown, and for these it was found that the sudden-freezing point was just upstream of the throat, at subsonic area ratios of 1.04 to 1.06 for all O/F values. It should be noted that in all cases experimental points are for the simulating gaseous reactants, but theoretical curves were calculated in terms of the storable propellants. The O/F abscissas correspond to the storable-propellant system. The O/F values for the experimental points were calculated from the flow rates and oxidant preheat values and represent the storable-propellant O/F corresponding most closely to the experimental conditions. Results on each plot summarize runs taken over a range of simulated O/F values within about 5 percent of the stated nominal O/F.

A typical plot of nozzle static-pressure measurements is shown in figure 5 for a run at a combustion-chamber pressure of 3.8×10^5 newtons per square meter and a simulated O/F of 2.05. The theoretical curves of equilibrium and frozen expansion for the corresponding storable propellants are also included. The kinetic calculation is omitted for clarity; this curve would nearly coincide with the frozen-expansion curve except at the highest area ratios. The experimental points lie between the limiting theoretical curves and somewhat closer to the frozen curve. Differences in pressure between equilibrium and frozen expansions are small enough that static pressure is an inaccurate parameter for conclusive studies of nonequilibrium expansion.

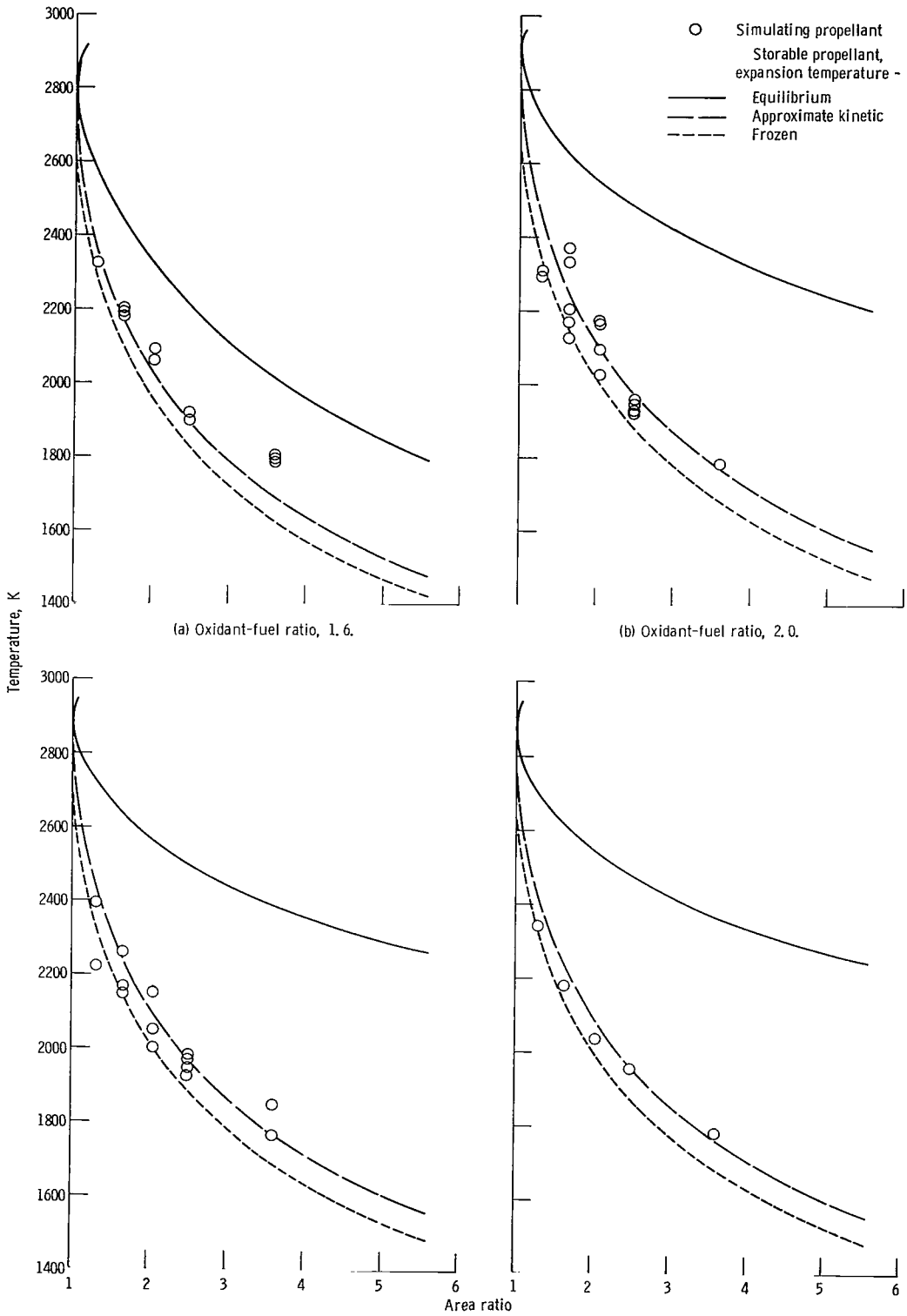

(a) Oxidant-fuel ratio, 1.6.

(b) Oxidant-fuel ratio, 2.0.

(c) Oxidant-fuel ratio, 2.25 (stoichiometric).

(d) Oxidant-fuel ratio, 2.4.

Figure 4. - Nozzle static temperatures at combustion-chamber pressure of 3.8×10^5 newtons per square meter (3.7 atm).

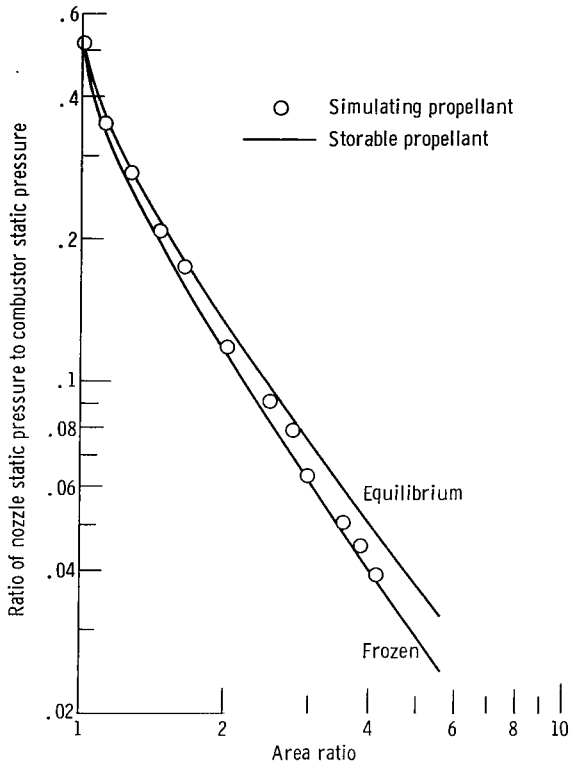

Figure 5. - Nozzle static pressures. Combustion-chamber pressure, 3.8×10^5 newtons per square meter; oxidant-fuel ratio, 2.05.

Effect of Combustion-Chamber Pressure

The effect of combustion-chamber pressure was not studied systematically in this investigation, but some runs were conducted at 4.8×10^5 newtons per square meter (4.7 atm) in addition to the majority at 3.8×10^5 newtons per square meter. An example of static temperature measurements at 4.8×10^5 newtons per square meter and a simulated O/F of 2.0 is shown in figure 6. The trends and general appearance of the data are identical to those at 3.8×10^5 newtons per square meter, although there was a slight increase, about 30 K, in the temperature levels of the calculated frozen and kinetic expansions.

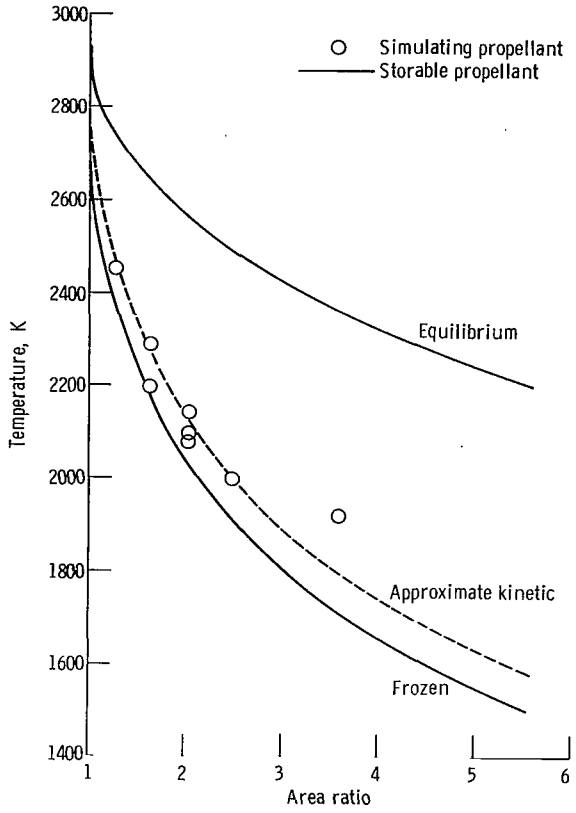

Figure 6. - Nozzle static temperatures. Combustion-chamber pressure, 4.8×10^5 newtons per square meter (4.7 atm); oxidant-fuel ratio, 2.0.

Effect of Oxidant-Fuel Ratio

Figures 7(a) to (d) and 8(a) to (c) show the temperature measurements as a function of simulated O/F at each optical station in the nozzle for combustion at 3.8×10^5 and 4.8×10^5 newtons per square meter. These figures include data shown as functions of area ratio in figures 4 and 6 plus additional measurements at intermediate O/F values not included previously. The theoretical curves for the storable propellants are also shown in figures 7 and 8. Because of limited or doubtful data, plots at area ratios of 2.50 and 3.60 for the 4.8×10^5 pressure and at an area ratio of 1.30 for the 3.8×10^5 pressure are not included. In general the measured temperatures are nearly independent of O/F, with a flat maximum and some dropoff at extreme values of O/F.

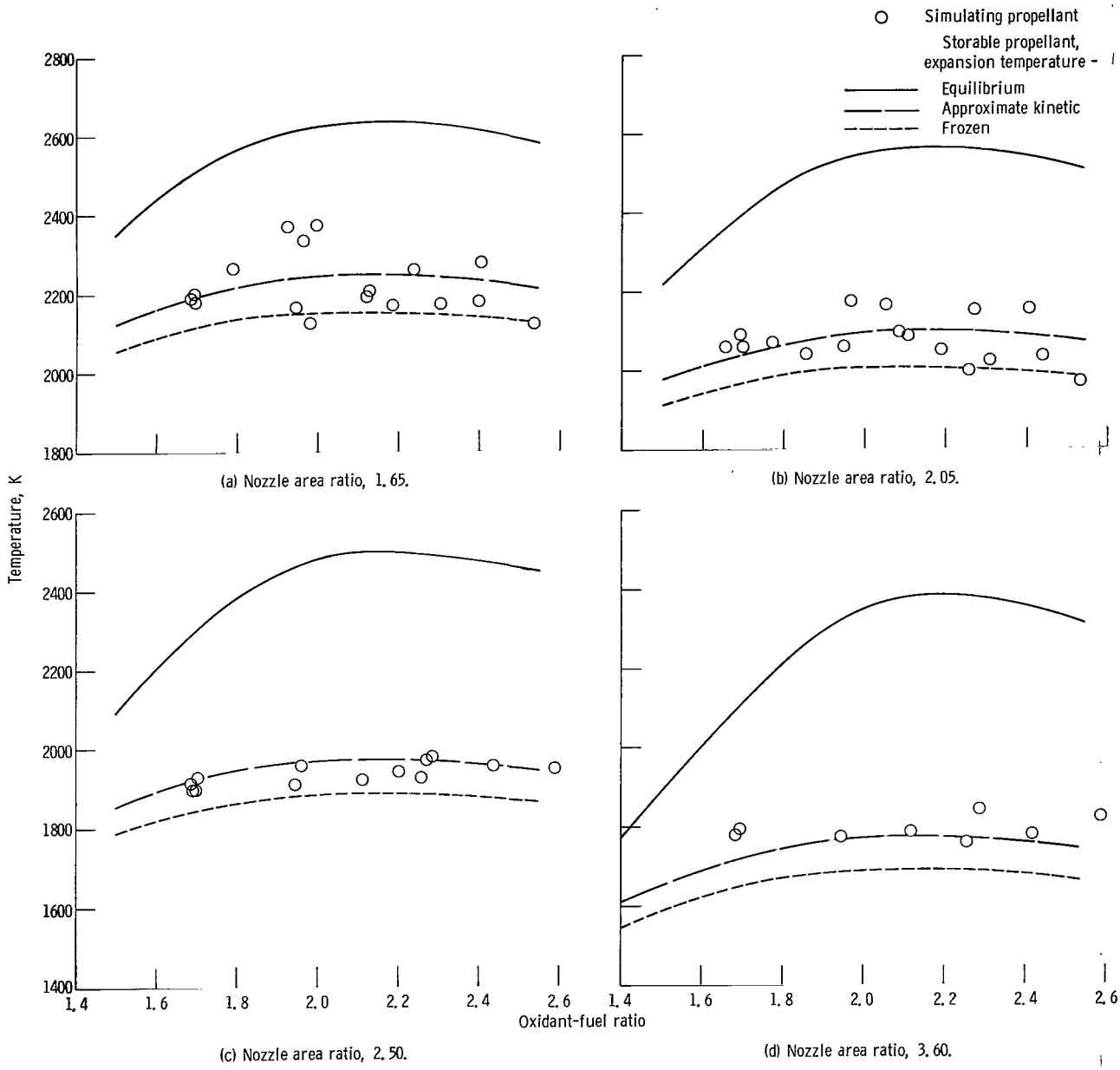

Figure 7. - Effect of oxidant-fuel ratio on nozzle static temperature at combustion-chamber pressure of 3.8×10^5 newtons per square meter.

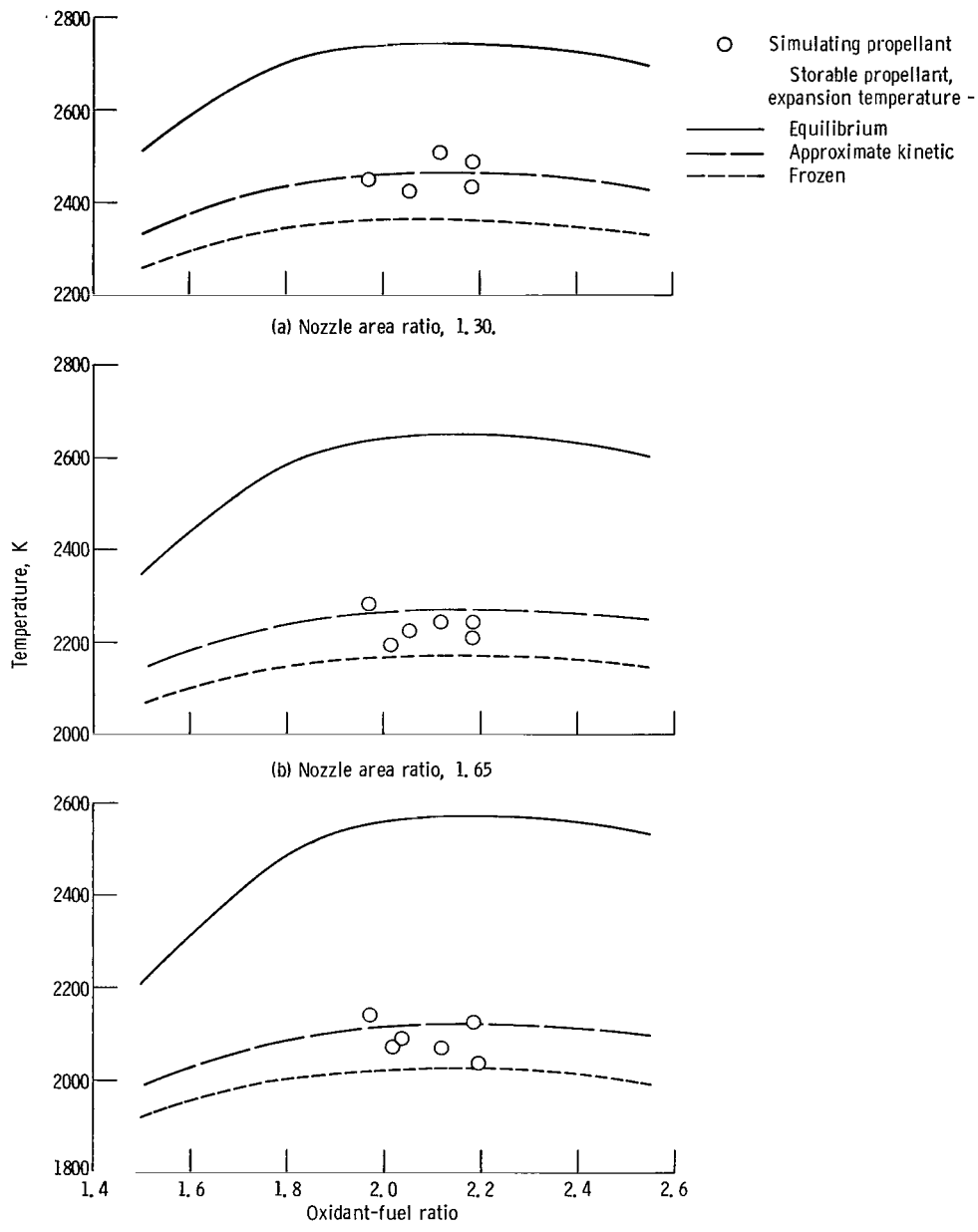

(a) Nozzle area ratio, 1.30.

(b) Nozzle area ratio, 1.65

(c) Nozzle area ratio, 2.05.

Figure 8. - Effect of oxidant-fuel ratio on nozzle static temperature at combustion-chamber pressure of 4.8×10^5 newtons per square meter.

DISCUSSION

Experimental Errors

The data scatter fell generally within a band of 50 K. Some imprecision is inherent in the reversal pyrometer method, due to window-transmission shifts, balancing drift, and temporal and spatial temperature fluctuations, as discussed in part in references 12 and 18. Additional sources of errors arose from possible misalinement of the optical axis and from nonuniform and fluctuating sodium carbonate distribution.

Possible errors in the definition of oxidant-fuel ratio due to off-simulation and the uncertainty of measured temperature at given nozzle locations due to two-dimensional temperature gradients are discussed in more detail in the following sections.

"Off-Simulation" Effects

The experimental operations introduced errors in the simulation, even where theory showed exact duplication was expected. A simulation at a desired O/F value required control of the composition of the fuel mixture, the preheat of the oxidant, and the relative flows of fuel, oxygen, and air. Each batch of fuel blend would vary slightly from the desired composition and consequently had a carbon-hydrogen ratio different from that required for the simulated hydrazine and UDMH fuel and nitrogen tetroxide oxidizer combustion. The fuel mixture therefore simulated the storable propellants with a small excess of carbon or hydrogen, as the case may be. To determine the influence of inaccurate fuel blending on nozzle-expansion results, theoretical calculations were made for some hypothetical situations. In figure 9(a), for example, temperatures are compared for the expansion of the products obtained with a fuel blend with excess carbon (expressed as a molecular weight 7 percent too high) and the desired expansion of storable-propellant products. Equilibrium- and frozen-expansion temperatures for these two cases are shown in figure 9(a) as a function of O/F at an area ratio of 2.05. This plot is analogous to the data presentation in figure 7(b).

Additional deviations from correct simulation conditions could arise from the setting of the oxidant-inlet temperature. Because the storage-heater outlet temperature was difficult to control precisely, it was expedient to operate a series of runs at a fixed oxidant-inlet temperature. This temperature could be correct for no more than one of a series of runs at different simulated O/F values, since oxidant-inlet temperature is a function of O/F. Theoretical calculations were made to determine the effect of incorrect oxidant-inlet temperature on results. The results presented in figure 9(b) compare the nozzle temperatures at an area ratio of 2.05 for expansion of the products of the simu-

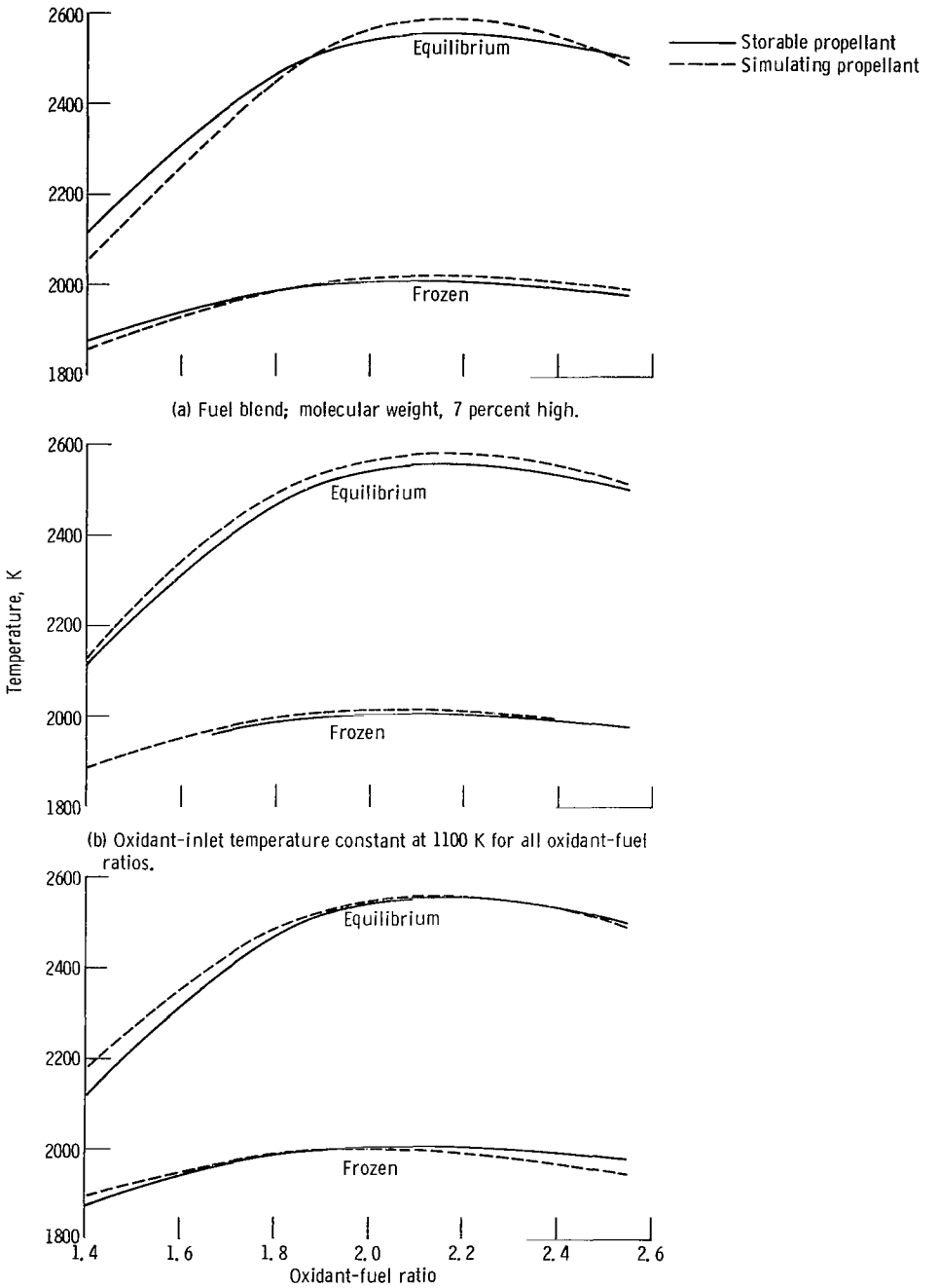

(a) Fuel blend; molecular weight, 7 percent high.

(b) Oxidant-inlet temperature constant at 1100 K for all oxidant-fuel ratios.

(c) Airflow, 10 percent high.

Figure 9. - Comparison between calculated nozzle temperatures for simulating propellants with prescribed errors and those for storable propellants. Combustion-chamber pressure, 3.8×10^5 newtons per square meter; area ratio, 2.05.

lating propellants with the oxidant-inlet temperature fixed at 1100 K, which is the correct value only at a simulated O/F of 1.65, with the corresponding storable-propellant product expansion.

Finally, the relative flows of fuel, oxygen, and air could not correspond always to exact values required for simulation. At best, the measured flows would simulate combustion at a storable-propellant O/F with some excess reactants, such as methane-hydrogen, oxygen, or air, which had no counterparts in the storable-propellant system. For convenience, a run was always arbitrarily characterized as simulating a storable-propellant O/F calculated from the carbon, oxygen, and hydrogen atoms supplied by the fuel and oxygen, with the misadjustments in flow rates expressed as an excess or deficiency in nitrogen atoms. Hence, the airflow rate, supplying the nitrogen atoms, was determined to be too large or too small as required. Runs where this airflow correction was great would have an inaccurate simulation. The effect of this flow-rate error was also calculated, and an example of this is illustrated in figure 9(c). There nozzle temperatures are shown for the expansion of storable-propellant combustion products and for simulating-propellant combustion products with reactant composition correct except for an airflow rate 10 percent low.

The cases presented in figures 9(a) to (c) illustrate effect of "off simulation," exaggerated to the extent that they represent greater tolerances than permitted in the experimental work. Additional calculations were made to determine effects of other off-simulation possibilities at varying operating conditions. In general, it was noted that the effect of these anticipated off-simulation variations on the nozzle temperatures was negligibly small, particularly where the expansion was near frozen. It was recognized that simulation of different conditions, such as other combustion-chamber pressures or wider O/F ranges, would possibly increase the sensitivity to these errors, and tighter control of simulation parameters would be required.

Two-Dimensional Effects

The theoretical analyses, as well as the interpretation of the experimental data, assume one-dimensional flow; that is, all properties are considered to be constant normal to the nozzle axis and to vary only in the axial direction. In the diverging portion of an axisymmetric nozzle, such an assumption is at best an approximation of the true flow field and can lead to inaccuracies in temperature predictions.

A two-dimensional flow field was calculated and is plotted in figure 10, where isothermal contour surfaces in the diverging portion of the nozzle are shown for frozen expansion of the storable-propellant products at an O/F of 2.0. The nozzle "walls" shown on this figure are the calibrated boundaries as mentioned in the APPARATUS sec-

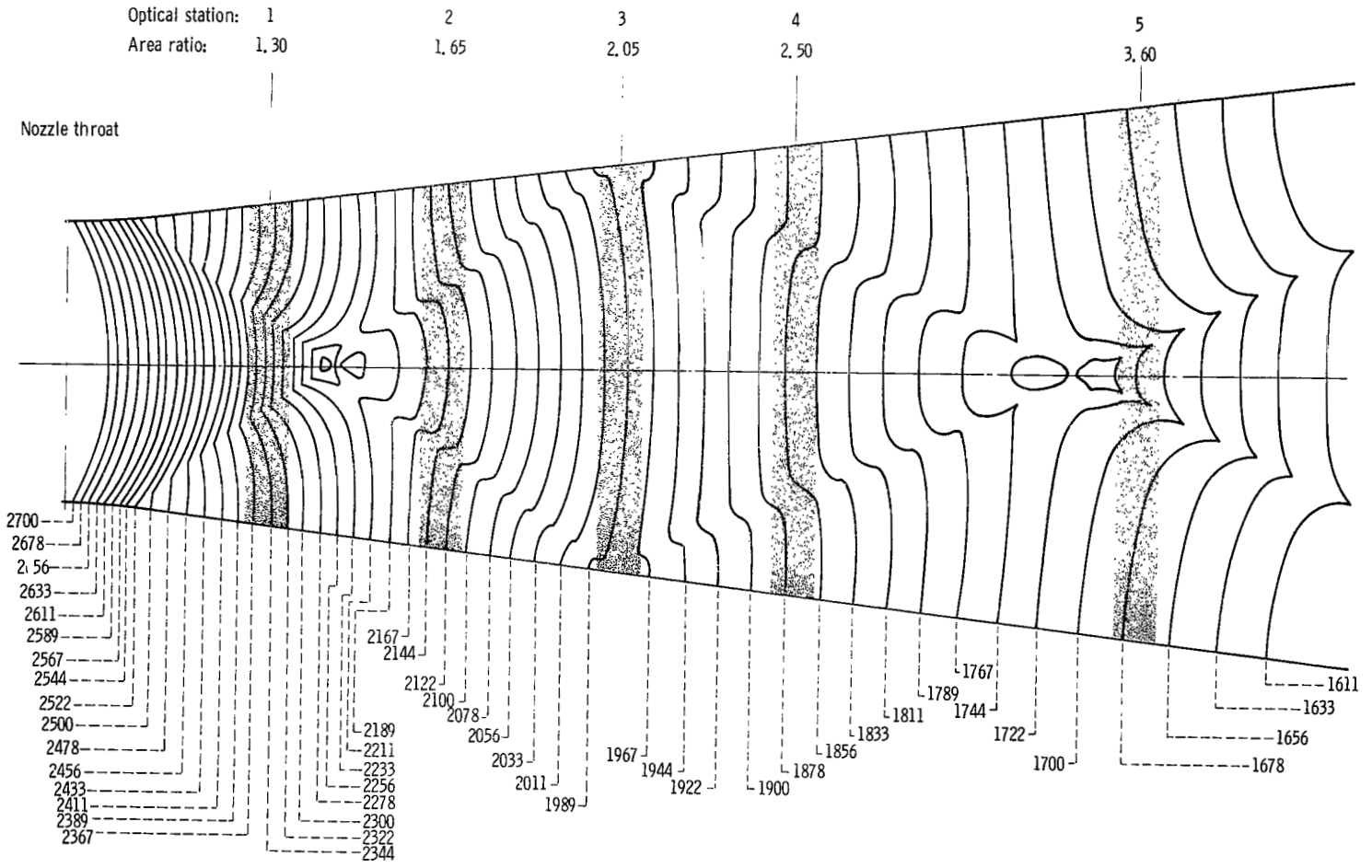

Figure 10. - Calculated isothermal contours in nozzle for frozen expansion of storable-propellant products. Combustion-chamber pressure, 3.8×10^5 newtons per square meter; oxidant-fuel ratio, 2.0.

tion, and the cooled boundary layer lies partly outside these walls and is omitted from the figure. Precise agreement with the data would, of course, require a two-dimensional kinetic plot, but the experimental data indicated expansion close to frozen, and a convenient method-of-characteristics program (ref. 19) was available to compute the frozen contours. The transonic isotherms are curved surfaces of revolution, as expected (ref. 20). In the conical nozzle downstream of the circular-arc throat, wave systems alter the transonic isothermal surfaces, smoothing the contours in some parts of the nozzle and distorting them in other parts. Reversal contours, where waves intersect at the centerline, result from computational inaccuracies and may not represent the true physical contours in these regions.

The shaded areas in figure 10 indicate the portions of the nozzle that can be observed through the optical windows; axial gradients across these windows are as much as 100 K, for example, at the 1.30-area-ratio station. Reproducibility of the reversal pyrometer readings would therefore be highly dependent on the axial positioning and slit alinement within the aperture defined by the window. Temperatures also vary radially along the optical path at each station because of the curved and distorted isothermal surfaces. Predicted one-dimensional temperatures are nominally the values near the wall. But it is likely that the reversal pyrometer measurements are influenced mainly by the centerline temperatures, particularly at the lower area ratios, since the spread of sodium seeding is probably confined to the central regions of the flow. In addition, measurements of reversal temperatures made in nonisothermal fields tend toward the maximum rather than average values because of the nonlinear response of this instrument with respect to temperature. The curved isothermal contours can therefore be responsible for some of the apparent inaccuracy of the data with respect to one-dimensional predictions at certain area ratios. Static-pressure profiles, such as figure 5, which consistently have points varying slightly above and below a smooth profile, are most likely caused by shock-wall (or shock-boundary layer) intersections.

Craig (ref. 21) presents some kinetic two-dimensional results for the hydrogen-air system in the 10.5° half-angle conical nozzle used in previous Lewis expansion studies (ref. 10). Craig notes "kinks" in wall pressure distribution, which correspond to changes in the spacing of the contours of pressure (or temperature, as plotted in fig. 10).

Comparisons with Analyses

For a few of the test conditions, data were compared to "exact" kinetic-expansion analyses for the storable-propellant system, such as those of reference 5. An exact kinetic calculation numerically solves the gas dynamic and chemical reaction-rate equations simultaneously for the expanding combustion products. Such a theoretical kinetic

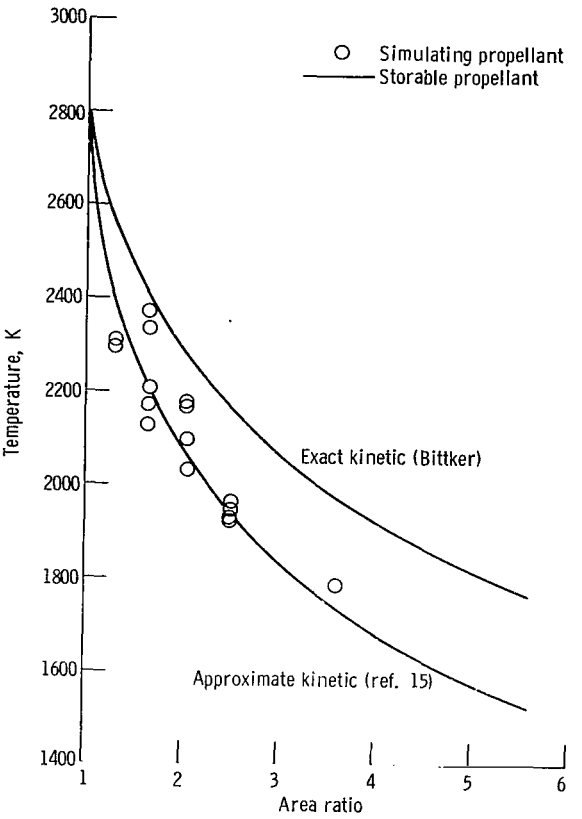

Figure 11. - Comparison of kinetic analyses with data. Combustion-chamber pressure, 3.8×10^5 newtons per square meter; oxidant-fuel ratio, 2.0.

curve for an O/F of 2.0 was calculated by David A. Bittker of Lewis and is presented in figure 11 along with the simulated-propellant data. The theoretical curve lies above all the data, although relative agreement is reasonable. The sudden-freezing approximate kinetic analysis (ref. 15), also shown in figure 11, is a better fit to the data. For consistency, this approximate analysis was modified by the use of reaction rates identical to those supplied to the exact kinetic program, instead of the rates quoted in the ANALYSIS section. But this curve is practically identical to that presented in figure 4(b). Both analyses are based on one-dimensional flow assumptions. The higher temperatures of the exact analysis with respect to the approximate sudden-freezing analysis appear to be the usual finding for the storable-propellant system (refs. 5 and 15). In general, the experimental and analytical temperatures are close enough to be considered in reasonable agreement.

Specific Impulse Calculations

To evaluate engine kinetic losses, vacuum specific impulse was calculated from the experimental data by linear interpolation between the equilibrium and frozen predictions obtained from the analytical programs. The ratio of experimental to equilibrium and frozen temperatures was used, as follows

$$I = I_{froz} + \frac{T_{exp} - T_{froz}}{T_{eq} - T_{froz}} (I_{eq} - I_{froz})$$

where I is specific impulse; T is temperature; and the subscript exp denotes experimental values, eq calculated equilibrium values, and froz calculated frozen values. An example of specific impulse values is plotted in figure 12, calculated for an area ratio of 3.6. While combustion pressures in this study were nearly representative, the ex-

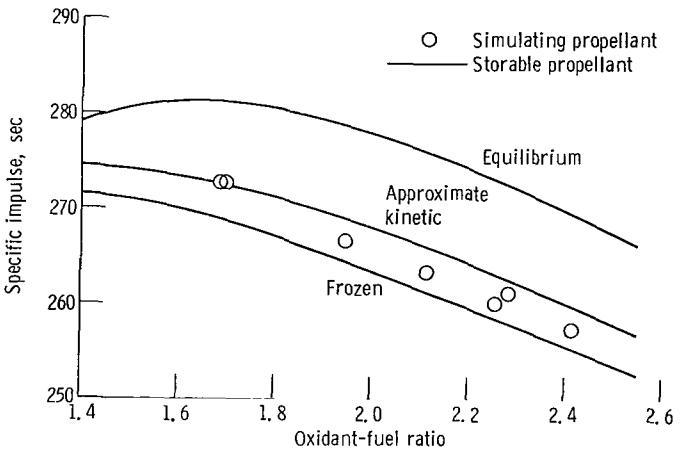

Figure 12. - Vacuum specific impulse. Combustion-chamber pressure, 3.8×10^5 newtons per square meter; area ratio, 3.60.

pansion is to a considerably smaller area ratio than those of 40 to 60 for typical storable-propellant engines (ref. 6). Hence, absolute values of specific impulse shown in figure 12 are low. The data at low area ratios are nevertheless useful in establishing the magnitude of kinetic losses. And extrapolation from these area ratios to higher area ratios is readily performed by using approximate kinetic, or more simply, frozen-expansion relations. Engine performance predictions, of course, must take into account combustion and aerodynamic losses, but the major degradation of performance of high-area-ratio, storable-propellant rockets can be shown to be the result of nonequilibrium expansion (ref. 6).

SUMMARY OF RESULTS

Investigation of the nonequilibrium expansion of the combustion products of the storable-propellant system, 50-weight-percent hydrazine and 50-percent UDMH fuel with nitrogen tetroxide oxidizer, was conducted at 3.8×10^5 and 4.8×10^5 newtons per square meter (3.7 and 4.7 atm) in a 5.6-area-ratio, nominal Mach 3, axisymmetric conical nozzle. The combustion products of the liquid storable propellants were simulated by combustion of gaseous methane, hydrogen, oxygen, and nitrogen to simplify combustion and confine the experimental problems to the expansion of the combustion products. Thermochemical calculations were made to relate the desired storable-propellant combustion products to the required flows and temperatures of the simulating reactants. Experimental measurements were made of static temperature and pressure of the expanding combustion products in the nozzle. Two principal results are summarized as follows:

1. The simulation of the storable propellants by the gases proved feasible. The calculation of the simulation assumed that the combustion reactions were in chemical equilibrium, and measurements of combustion temperature confirmed that this assumption was correct for this set of reactants. In practice, it was necessary to permit variations of propellant flow rates and inlet temperatures from those values theoretically required. Calculations, however, showed that the influence of "off-simulation" conditions on nozzle temperatures would be very small for the range of this study.

2. Experimental static temperatures for expanding combustion products, simulating oxidant-fuel mass ratios (O/F) of 1.6 to 2.5 (equivalence ratios of 1.4 to 0.9) were nearly independent of O/F and were close to the temperatures predicted for frozen expansion. Results at combustion-chamber pressures of 3.8×10^5 and 4.8×10^5 newtons per square meter (3.7 and 4.7 atm) were nearly identical, although due to the small change in pressure this result is not unexpected. The data agreed fairly well with an exact kinetic analysis, based on a "sudden-freezing" assumption. Calculations were presented showing the theoretical two-dimensional flow field, and qualitative observations were made concerning errors introduced by a one-dimensional assumption. Specific impulse values derived from the experimental data were also presented.

Lewis Research Center,
National Aeronautics and Space Administration,
Cleveland, Ohio, June 18, 1969,
722-03-00-03-22.

REFERENCES

1. Lezberg, Erwin A.; and Franciscus, Leo C.: Effects of Exhaust Nozzle Recombination on Hypersonic Ramjet Performance: I. Experimental Measurements. AIAA J., vol. 1, no. 9, Sept. 1963, pp. 2071-2076.

2. Lezberg, Erwin A.; Rose, Charles M.; and Friedman, Robert: Comparisons of Experimental Hydroxyl Radical Profiles with Kinetic Calculations in a Supersonic Nozzle. NASA TN D-2883, 1965.

3. Simkin, D. J.; and Koppang, R. R.: Recombination Losses in Rocket Nozzles with Storable Propellants. AIAA J., vol. 1, no. 9, Sept. 1963, pp. 2150-2152.

4. Wilde, Kenneth A.: Complex Kinetics in Adiabatic Flow: C - H - O (N) Systems. AIAA J., vol. 3, no. 10, Oct. 1965, pp. 1846-1849.

5. Burwell, W. G.; Sarli, V. J.; and Zupnik, T. F.: Applicability of Sudden-Freezing Criteria in Analysis of Chemically Complex Rocket Nozzle Expansions. Recent Advances in Aerothermochemistry. Vol. 2. I. Glassman, ed., AGARD Conference Proc. No. 12, Vol. II, 1967, pp. 701-759.

6. Aukerman, Carl A.; and Trout, Arthur M.: Experimental Rocket Performance of Apollo Storable Propellants in Engines with Large Area Ratio Nozzles. NASA TN D-3566, 1966.

7. Sheeran, W.: Simulation of Earth-Storable Liquid Propellants with Gaseous Reactants. Rep. HFD-PS-67-5, Cornell Aeros., Lab., Inc., June 1967.

8. Just, Th.; and Pippert, H.: Measurements of Relaxation Effects in Nozzle Flow of Hot Combustion Gases by Means of a Shock Tube Technique II. Recent Advances in Aerothermochemistry. Vol. 2. I. Glassman, ed., AGARD Conference Proc. No. 12, Vol. II, 1967, pp. 761-776.

9. Lancashire, R. B.; Lezberg, E. A.; and Morris, J. F.: Heat-Transfer Coefficients for a Full-Scale Pebble-Bed Heater. Ind. Eng. Chem., vol. 52, no. 5, May 1960, pp. 433-434.

10. Lezberg, Erwin A.; and Lancashire, Richard B.: Expansion of Hydrogen-Air Combustion Products through a Supersonic Exhaust Nozzle; Measurements of Static-Pressure and Temperature Profiles. Combustion and Propulsion, Fourth AGARD Colloquium. A. L. Jaumotte, A. H. Lefebvre and A. M. Rothrock, eds., Pergamon Press, 1961, pp. 286-305.

11. Buchele, Donald: A Self-Balancing Line-Reversal Pyrometer. Temperature - Its Measurement and Control in Science and Industry. Vol. 3, Part 2. A. I. Dahl, ed., Reinhold Publ. Corp., 1962, pp. 879-887.

12. Lezberg, Erwin A.; and Buchele, Donald R.: Some Optical Techniques for Temperature and Concentration Measurements of Combustion in Supersonic Streams. NASA TN D-2441, 1964.

13. Zeleznik, Frank J.; and Gordon, Sanford: A General IBM 704 or 7090 Computer Program for Computation of Chemical Equilibrium Compositions, Rocket Performance, and Chapman-Jouguet Detonations. NASA TN D-1454, 1962.

14. Sawyer, Robert F.: Theoretical Effect of Nonequilibrium Combustion on N_2H_4/N_2O_4 Propellant Performance. J. Spacecraft Rockets, vol. 5, no. 1, Jan. 1968, pp. 116-117.

15. Franciscus, Leo C.; and Healy, Jeanne A.: Computer Program for Determining Effects of Chemical Kinetics on Exhaust-Nozzle Performance. NASA TN D-4144, 1967.

16. Franciscus, Leo C.; and Lezberg, Erwin A.: Effects of Exhaust Nozzle Recombination on Hypersonic Ramjet Performance: II. Analytical Investigation. AIAA J., vol. 1, no. 9, Sept., 1963, pp. 2077-2083.

17. Getzinger, Richard W.: A Shock-Wave Study of Recombination in Near-Stoichiometric Hydrogen-Oxygen Mixtures. Eleventh Symposium (International) on Combustion. Combustion Institute, Pittsburgh, Pa., 1967, pp. 117-124.

18. Buchele, Donald R.: Nonlinear-Averaging Errors in Radiation Pyrometry. NASA TN D-2406, 1964.

19. Thompson, D.; Ingram, E. H.; Young, C. T. K.; and Cox, J. B.: A FORTRAN Program to Calculate the Flow Field and Performance of an Axially Symmetric deLaval Nozzle. NASA TN D-2579, 1965.

20. Kliegel, James R.; and Quan, Victor: Convergent-Divergent Nozzle Flows. AIAA J., vol. 6, no. 9, Sept. 1968, pp. 1728-1734.

21. Craig, Roger R.: Applying the Method of Characteristics to Analyze the Flow Field of a Chemically Reacting Gas in a Two Dimensional or an Axisymmetric Nozzle. Rep. AFAPL-TR-65-20, Air Force Systems Command, Apr. 1965. (Available from DDC as AD-618068.)

NATIONAL AERONAUTICS AND SPACE ADMINISTRATION
WASHINGTON, D.C. 20546
OFFICIAL BUSINESS

FIRST CLASS MAIL

POSTAGE AND FEES PAID
NATIONAL AERONAUTICS AND
SPACE ADMINISTRATION

POSTMASTER: If Undeliverable (Section 158 Postal Manual) Do Not Return

"The aeronautical and space activities of the United States shall be conducted so as to contribute . . . to the expansion of human knowledge of phenomena in the atmosphere and space. The Administration shall provide for the widest practicable and appropriate dissemination of information concerning its activities and the results thereof."

—NATIONAL AERONAUTICS AND SPACE ACT OF 1958

NASA SCIENTIFIC AND TECHNICAL PUBLICATIONS

TECHNICAL REPORTS: Scientific and technical information considered important, complete, and a lasting contribution to existing knowledge.

TECHNICAL NOTES: Information less broad in scope but nevertheless of importance as a contribution to existing knowledge.

TECHNICAL MEMORANDUMS: Information receiving limited distribution because of preliminary data, security classification, or other reasons.

CONTRACTOR REPORTS: Scientific and technical information generated under a NASA contract or grant and considered an important contribution to existing knowledge.

TECHNICAL TRANSLATIONS: Information published in a foreign language considered to merit NASA distribution in English.

SPECIAL PUBLICATIONS: Information derived from or of value to NASA activities. Publications include conference proceedings, monographs, data compilations, handbooks, sourcebooks, and special bibliographies.

TECHNOLOGY UTILIZATION PUBLICATIONS: Information on technology used by NASA that may be of particular interest in commercial and other non-aerospace applications. Publications include Tech Briefs, Technology Utilization Reports and Notes, and Technology Surveys.

Details on the availability of these publications may be obtained from:

SCIENTIFIC AND TECHNICAL INFORMATION DIVISION

NATIONAL AERONAUTICS AND SPACE ADMINISTRATION

Washington, D.C. 20546